Journal of Applied Polymer Science

Surface Molecularly Imprinted Polymers Based on Yeast Prepared by Atom Transfer Radical Emulsion Polymerization for Selective Recognition of Ciprofloxacin from Aqueous Medium

Juan Wang,[1] Jiangdong Dai,[2] Minjia Meng,[1] Zhilong Song,[1] Jianming Pan,[1] Yongsheng Yan,[1] Chunxiang Li[1]

[1]School of Chemistry and Chemical Engineering, Jiangsu University, Zhenjiang 212013, China
[2]School of Material Science and Engineering, Jiangsu University, Zhenjiang 212013, China
Correspondence to: C. Li (E-mail: lichunxiang202@163.com)

ABSTRACT: To achieve selective recognition of water-soluble ciprofloxacin (CIP), an effective method was developed for the preparation of surface molecularly imprinted polymers based on the yeast particles (yeast@MIPs) via atom transfer radical emulsion polymerization (ATREP). The reactions were carried out in the nontoxic and green emulsion system at room temperature, which was environment friendly with low energy consumption. In this study, the yeast, for the advantages of low cost, easily available source and abundant active groups on the cell wall, was selected as an ideal biological support substrate. The prepared yeast@MIPs was characterized by FT-IR, SEM, TEM, EDS, and elemental analysis techniques. Batch mode adsorption studies were carried out to investigate the specific adsorption equilibrium, kinetics, selective recognition, and reuse ability of yeast@MIPs. The experimental static adsorption data of CIP on to yeast@MIPs were well-described by Langmuir, Freundlich, and pseudo-second-order models. The maximum static adsorption capacity for CIP of yeast@MIPs was 18.48 mg g^{-1}, and the adsorption equilibrium could be reached in 60 min. The selectivity coefficients for CIP relative to enrofloxacin, tetracycline, and sulfadiazine were 1.212, 2.002, and 10.65, which demonstrated CIP of high affinity and selectivity over three competitive antibiotics. In addition, the reusability of the material without obvious deterioration (8.52% loss) in performance was observed at least four repeated cycles. And the yeast@MIPs was used to determine CIP from spiked shrimp samples by HPLC analysis. These results showed that yeast was a well-defined substrate and ATREP was a promising technique for the preparation of surface molecularly imprinted polymers targeting templates. © 2013 Wiley Periodicals, Inc. J. Appl. Polym. Sci. **2014**, *131*, 40310.

KEYWORDS: adsorption; molecular recognition; kinetics; separation techniques; emulsion polymerization

Received 26 July 2013; accepted 16 December 2013
DOI: 10.1002/app.40310

INTRODUCTION

Ciprofloxacin (CIP) is a third-generation fluoroquinolone antimicrobial with a broad spectrum of activity against a wide range of bacterial infections.[1–4] Easy to use, low cost, and distinct curative effect, all these advantages impel CIP to become one of the most commonly used antibiotics all the time.[5] Although CIP is an extensively applied antibiotic, its residue can be detected in animal products and water resources, which may cause a potential threat to human health.[6,7] Therefore, it is urgently required to resolve the increasingly prominent issue and develop an efficient and inexpensive treatment method for the selective recognition and removal of target antibiotic from the environmental pollutants.[8,9] Until now, the analytical methods for CIP mostly focus on chromatography separation, such as high-performance liquid chromatography (HPLC),[10] capillary electrophoresis,[11] and spectrophotometry.[12] However, these methods are time-consuming and require a tedious sample pretreatment. Therefore, the great priority has been given to the development of novel molecular recognition and selective separation techniques. Over the past decades, molecular imprinting technique (MIT) has received considerable attention with overwhelming superiority, such as higher reusability, selectivity, and lower consumption.[13–15] MIT is a facile, well-established approach to prepare molecularly imprinted polymers (MIPs) by the copolymerization of functional and crosslinking monomers in the presence of template molecules. Subsequent removal of template molecules from the polymer matrix generates tailor-made recognition sites, which are complementary in shape, size, and functionality of the template molecules.[16]

Additional Supporting Information may be found in the online version of this article.

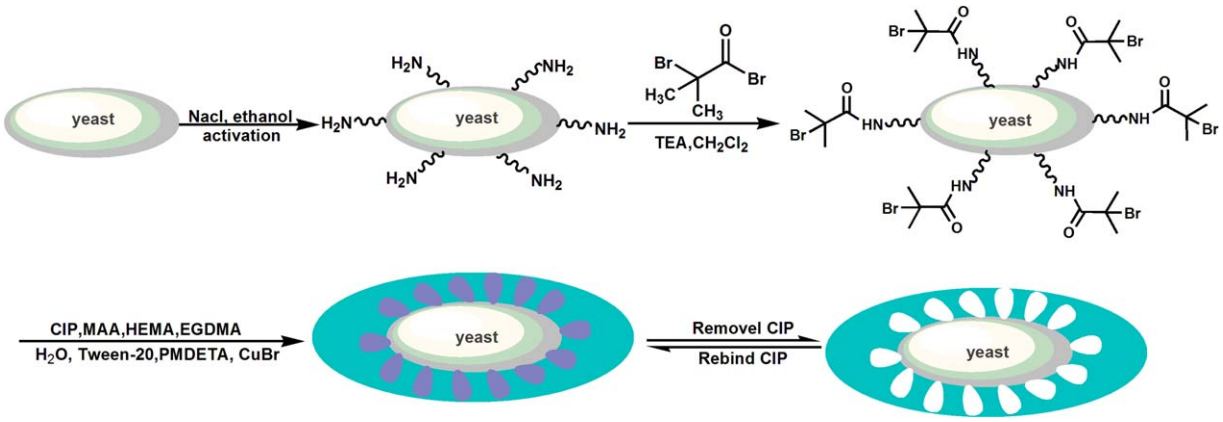

Figure 1. Schematic route of yeast@MIPs prepared via ATREP. [Color figure can be viewed in the online issue, which is available at wileyonlinelibrary.com.]

To our knowledge, traditional preparation methods had not achieve the full potential of MIPs with the limitations unsolved, such as poor site accessibility and low binding capacity.[17] Some efforts have been made to address these problems proposed, such as surface/film imprinting,[18–20] surface graft imprinting,[21] and surface core-shell nanoparticles.[22] All these materials have in common are to prepare MIPs at the surface or in the proximity of materials surface; namely, surface molecularly imprinted polymers, which facilitate the complete removal of templates and provide higher binding capacity and faster mass transfer.[7] The choice of support substrates, with excellent morphology and mechanical properties, is crucial for preparing the surface molecularly imprinted polymers. As we know, the conventional substrates used for surface imprinting technique are silica gel,[23] graphene,[24] and Fe_3O_4 nanoparticles[9], etc. However, the intensity and compatibility between inorganic materials and imprinted polymer layer is low. In recent years, biological materials are applied to the preparation of molecularly imprinted polymers and have the potential to substitute for traditional imprinting matrix. For instance, Romana Schirhagl's team has investigated a double imprinting approach using the natural antibodies as template to generate biomimetic receptors and use them for detection of large biomolecules.[25,26] In this study, the yeast was selected as the matrix material, for its advantages of low cost, easily available source, and abundant functional groups, which makes it more conducive to form molecularly imprinted polymers layer on the yeast surface.

Atom transfer radical polymerization (ATRP), as a new class of controlled living radical polymerization (CRP), has rapidly attracted increasing interest because of its high tolerance toward a wide range of monomers, high compatibilities, and relatively mild reaction conditions.[27–29] Recently, ATRP has been proposed as a popular new surface imprinting technology successfully applied in many cases.[30] For instance, Wang et al. had prepared MIPs nanotube membrane with uniform pores and adjustable thickness by surface-initiated atom transfer radical polymerization (ATRP).[18] Lu and co-workers had provided a simple method to prepare superparamagnetic surface MIP core-shell nanoparticles via ATRP to get uniform thin MIPs layer.[31] However, most of the imprinting processes using ATRP were carried out in organic solvents, such as acetonitrile and chloroform, which are relatively expensive and toxic. It also remains a challenge to prepare MIPs by ATRP in green solvent, such as water, because the hydrogen bonding interaction between template and monomers can be interrupted by water.[32] Our group recently reported the preparation of imprinted polymers based on the yeast-supported ATRP in the binary mixture of methanol and water.[33,34] However, the resulting imprinted polymers by methanol–water system exhibited larger-sized, heterogeneous and thicker imprinting layer, in which the recognition sites were deeply embedded and that affected the adsorption capacity. For further research, we found that the emulsion system had the potential to solve these problems. The emulsion polymerization was carried out in aqueous phase with an emulsifier, in which the solvents are nontoxic and the resulting emulsion system is homogeneous.[35] In addition, the obtained MIPs by emulsion demonstrated uniform-sized, good dispersible performances and large adsorption capacity. Hence, ATRP emulsion polymerization was chosen to synthesize surface molecularly imprinted polymers in this work.

In this study, we made our first attempt to prepare surface imprinted polymer by ATREP using biological material yeast as substrate, which made it possible to recognize CIP from aqueous solution. First, the halogen was introduced on to the surface of the yeast to obtain the yeast@Br composites. Next, the yeast@Br composites were dispersed in the mixture of Tween-20 and water, and then the yeast@MIPs were prepared using CIP as the template, methacrylic acid (MAA), hydroxyethyl methacrylate (HEMA) as functional monomers and ethylene glycol dimethacrylate (EGDMA) as crosslinking agent, respectively. Finally, PMDETA and CuBr were added in the above mixture as the ATRP catalytic system, and then the polymerization was carried out at room temperature. The synthesis route of yeast@MIPs were illustrated in Figure 1, and the prepared yeast@MIPs were characterized by Fourier transform infrared spectroscopy (FT-IR), scanning electron microscope (SEM), transmission electron microscopy (TEM), elemental analysis, and energy dispersive X-ray spectrometer (EDS). The adsorption capacity, kinetics, selectivity, and reusability of the yeast@MIPs were also investigated in detail. The yeast@MIPs were also applied to determine CIP by HPLC analysis in real samples.

EXPERIMENTAL

Materials

Yeast powder was purchased from Angel Yeast Co. (Yichang, China). Sodium chloride (NaCl), triethylamine (TEA), methanol, ethanol, methacrylic acid (MAA), acetic acid, trichloroacetic acid, dichloromethane (CH_2Cl_2) and CuBr were obtained from Sinopharm Chemical Reagent Co. (Shanghai, China). *N*,*N*,*N*′,*N*″,*N*″-pentamethyl diethyenetriamine (PMDETA), 2-bromoisobutyryl bromide, polyoxyethylene-(20) sorbitan monolaurate (Tween-20) and ethylene glycol dimethacrylate (EGDMA) were obtained from Aladdin reagent Co. (Shanghai, China). Hydroxyethyl methacrylate (HEMA) was obtained from Adamas Reagent Co. (Shanghai, China). Ciprofloxacin (CIP), enrofloxacin (ENR), sulfadiazine (SMZ), and tetracycline (TC) were obtained from Mengyimei Shengwu Keji Co. (Beijing, China). Deionized water used throughout the experiments was obtained from laboratory purification system. The chemicals for high-performance liquid chromatography (HPLC) were at least of HPLC grade, other chemicals were analytical reagent grade.

Instrument

Infrared spectra (4000–400 cm^{-1}) were recorded on a Nicolet NEXUS-470 FTIR apparatus. The morphologies of yeast and yeast@MIPs were observed by a scanning electron microscope (SEM, JEOL, JSM-7001F) and a transmission electron microscope (TEM, JEOL, JEM-2100). UV–vis adsorption spectra were obtained with a UV–vis spectrophotometer (UV-2450, Shimadzu, Japan). A Vario EL elemental analyzer (Elementar, Hanau, Germany) was employed to investigate the elemental composition of the composites. Energy dispersive X-ray spectra (EDS) images were collected on an F20S-TWIN electron microscope (Tecnai G2, FEI Co.), using a 200 kV accelerating voltage. HPLC analysis was performed on a Shimadzu LC-20A system (Shimadzu, Kyoto, Japan) equipped with a UV–vis detector.

Synthesis of Yeast@Br Composites

First, 3.0 g of yeast was dissolved in 50 mL of 0.9 wt % NaCl aqueous solution under a vigorous stirring for 3.0 h at 35°C. Then, the yeast was collected by suction filtration and washed with ethanol till dry to get the activated yeast. Secondly, 2.0 g of activated yeast, 40 mL of CH_2Cl_2 and 3.0 mL of triethylamine were kept in the ice bath with the nitrogen protection for 30 min. 3.0 mL of 2-bromoisobutyryl bromide were added dropwise in the above solution. Subsequently, the mixture was reacted at room temperature (25°C) for 12 h. The obtained composites (designated yeast@Br) were collected and washed with CH_2Cl_2 and ethanol several times, and were finally dried at 50°C under vacuum for 12 h before use.

Synthesis of Yeast@MIPs by ATRP Emulsion Polymerization

Briefly, 0.5 g of Tween 20 was dissolved in three round-bottom flask containing 30 mL of water under a vigorous stirring at 35°C till no bubbles appeared. After that ciprofloxacin (0.125 mmol), HEMA (0.25 mmol), MAA (0.25 mmol), 0.2 g of yeast@Br and a certain amount of EGDMA were successively added in the above solution. The mixture was proceeded in an ultrasonic bath for 10 min to get the preassemble solution. Moreover, 25 μL of PMDETA was slowly added into the above mixture after the flask's exchanging with nitrogen for 15 min. Finally, the reaction system was deoxygenated for 20 min by exchanging with nitrogen before 14.3 mg of CuBr was quickly injected into the flask. Then, the mixture was stirred and carried out at 35°C under N_2 protection for 24 h. After the polymerization, the product was collected by centrifugation and was dried at 35°C under vacuum for 12 h. Then, the resulting surface imprinted particles (designated yeast@MIPs) were washed with the mixture solution of 100 mL methanol/acetic acid (9:1, v/v) using Soxhlet extraction to remove the template molecule. The yeast@MIPs was dried in a vacuum oven at 60°C overnight. In comparison, nonimprinted polymers (yeast@NIPs) were also prepared by a parallel way, but with the ciprofloxacin omitting. Meanwhile, the molecularly imprinted polymers by ATREP (designated MIPs) without the based yeast particles were synthesized in the same way. In addition, the preparation conditions of yeast@MIPs were optimized by varying the amount of EGDMA.

Batch Binding Experiment Studies

Commonly, investigation on static binding behaviors of synthetic imprinted polymers should be determined by isothermal adsorption and adsorption kinetics studies in a batch mode of experiments. In adsorption isotherm studies: 5.0 mg of yeast@MIPs or yeast@NIPs was added into 10 mL different initial CIP concentrations ranging from 5.0 to 200 mg L^{-1}. Then, the solutions were stirred 10 min and kept stable overnight at 298, 308, and 318 K, respectively.[36] The residual concentration of CIP in the aqueous solution was determined by the UV–vis spectrophotometer at 276 nm before the samples were centrifuged and the supernatant solution was collected. The equilibrium amount of CIP adsorbed on to the polymers (Q_e, mg g^{-1}) was calculated according to the following formula:

$$Q_e = \frac{(C_o - C_e)V}{W} \quad (1)$$

where C_o (mg L^{-1}) and C_e (mg L^{-1}) are the initial and the residual of the template solution concentrations, respectively. V (L) stands the solution volume and W (g) is the adsorbent mass. The tests were done in triplicate. Meanwhile, the isothermal adsorption experiments of the molecularly imprinted copolymer without based yeast (MIPs) were also investigated in the same conditions of yeast@MIPs.

In adsorption kinetic studies: the influences of equilibration time (5–360 min) on the adsorption of template were investigated. The initial CIP concentration was set as 100 mg L^{-1} and the batch kinetics studies were parallel to equilibrium tests. The amount adsorbed (Q_t, mg g^{-1}) was calculated according to the following equation:

$$Q_t = \frac{(C_0 - C_t)V}{m} \quad (2)$$

where C_t (mg L^{-1}) represents the concentration of CIP solution at time t.

Selective Recognition Experiments

To examine the selectivity of the yeast@MIPs, 5.0 mg of the yeast@MIPs or yeast@NIPs were added into colorimetric tubes, each of which contained 10 mL solution with 50 μmol L^{-1} of CIP, ENR, TC, and SMZ, respectively. The experiments were

Table I. Elemental Analysis of the Yeast and the Compounds Obtained

Samples	C (%)	H (%)	N (%)
Active yeast	46.30	7.29	8.40
Yeast@Br	45.27	6.98	2.40
Yeast@MIPs	53.79	7.36	3.61
Yeast@NIPs	53.06	7.45	3.09

carried out on a shaker at 298 K for 12 h. After adsorption, the binding amounts of yeast@MIPs and yeast@NIPs were calculated as the procedure of static adsorption studies.

The distribution coefficients (K_D), selectivity coefficients (k), and relative selectivity coefficients (k') of ENR, TC, and SMZ with respect to CIP can be obtained according to the following equations:

$$K_D = \frac{Q_e}{C_e} \tag{3}$$

$$k = \frac{K_{D(CIP)}}{K_{Dj}} \tag{4}$$

$$k' = \frac{k_M}{k_N} \tag{5}$$

where Q_e (μmol g^{-1}) and C_e (μmol L^{-1}) are the equilibrium binding amount and the equilibrium concentration of the CIP and competitive antibiotics, respectively. K_{Dj} represents the distribution coefficients of competition species. k_M and k_N are the selectivity coefficients of yeast@MIPs and yeast@NIPs, correspondingly.

Desorption and Reusability Experiments

The adsorption–desorption experiments were carried out to investigate the reuse property of yeast@MIPs. 5.0 mg of yeast@MIPs was firstly conducted according to the procedure of isothermal adsorption. Afterwards, a volume of 5.0 mL mixture of methanol and acetic acid (9:1, v/v) was added to almost elute all the CIP. Lastly, 5.0 mL distilled water was used to wash again to neutral condition for the next adsorption–desorption cycle. The experiments were repeated for 4.0 times and conducted at 308 K to get desired regeneration.

Determination of CIP in Shrimp Samples

To evaluate the potential application of yeast@MIPs in real sample analysis, 5 g of fresh shrimp samples were crushed into homogenate paste. Then, the homogenate paste was dispersed in 15% (w/v) trichloroacetic acid aqueous solution and the blended solution was stirred for 2 h at 398 K. After centrifugation and filtration, the extraction solution was collected and spiked with CIP at levels of 50 μg L^{-1}. 5 mg of yeast@MIPs or yeast@NIPs were dispersed in 10 mL of the spiked shrimp samples and then the mixtures were incubated in an incubator shaker for 6 h at 298 K. Subsequently, the yeast@MIPs or yeast@NIPs were collected by centrifugal filtration and washed with 10 mL methanol–acetic acid solution (v/v = 9 : 1). The extracts were dried using N_2 stream at 298 K and the residues were redissolved in 0.4 mL methanol for further HPLC analysis.

RESULTS AND DISCUSSION

Preparation Conditions Optimization of Yeast@MIPs

To obtain the higher adsorption capacity and better morphology of yeast@MIPs, the amount of crosslinker (EGDMA) was optimized. We had chosen the molar amounts of EGDMA about 0.5, 1.0, 1.5, 2.0, 2.5, 3.0 mmol. The rest of the conditions were kept the same. As shown in Supporting Information Figure S1, yeast@MIPs displayed six different morphologies as the usage amounts of EGDMA changed. In brief, when the molar amount was 0.5 mmol, the synthetic imprinted layer was not enough to cover all the surface of yeast. While 3.0 mmol EGDMA was used, the yeast particles were embedded in the thick imprinted polymers, which are almost invisible. Through the comparison of the six images, we found that Supporting Information Figure S1d appeared excellent morphology and dispersion, and the corresponding usage amount of EGDMA was 2.0 mmol. Meanwhile, the adsorption capability of varying crosslinker was shown in Support Information Figure S2, as the amount of EGDMA increasing, the adsorption capacity first increased significantly. This may be ascribed to enough vacant active sites on surface and the driving force of concentration gradient. However, the growth trend of CIP adsorption capacity was very ease when the usage amount of EGDMA arrived at 2.0 mmol. Through integrated into account, 2.0 mmol of EGDMA was the optimized condition to prepare surface molecularly imprinted polymers based on yeast.

Characterization of the Yeast@MIPs

The results of elemental analysis including each modification process were shown in Table I. Compared with active yeast, the decrease of each element composition of yeast@Br could be attributed to the introduction of halogen (Br) on to the surface of yeast.[37] After polymerization, it could be found that the carbon composition increased from 45.27 to 53.79% and 53.06% for yeast@MIPs and yeast@NIPs, and the hydrogen composition also increased from 6.98 to 7.36% and 7.45%, respectively. The results suggested that monomers HEMA and MAA (containing carboxylic groups) were successfully reacted with template. The difference of elemental compositions between yeast@MIPs and yeast@NIPs indicated that the template molecules were not able to be completely eluted from the MIPs.

To further determine the successful introduction of bromine on the surface of yeast, EDS detection was also carried out.[38] As shown in Figure 2, we could clearly observe a broad distinct peak of Br element composition in Figure 2(b), which did not appear in Figure 2(a). This phenomenon definitely proved that the presence of bromine in the modified yeast.

Morphological features of yeast and yeast@MIPs were characterized by SEM and TEM and the results were illustrated in Figure 3(a–d), respectively. It could be obtained from SEM image of Figure 3(a), yeast purchased commercially was smooth-faced ellipsoid shape with the uniform size. When compared with the crude yeast, the well-defined yeast@MIPs were monodispersed, plump, rough-faced shape, which could be obviously observed from Figure 3(b,c). The outer MIPs coating layer was shown from the TEM image [Figure 3(d)]. In the study, we calculated the mean diameter of the particles based on a weighted-averages method through measurement

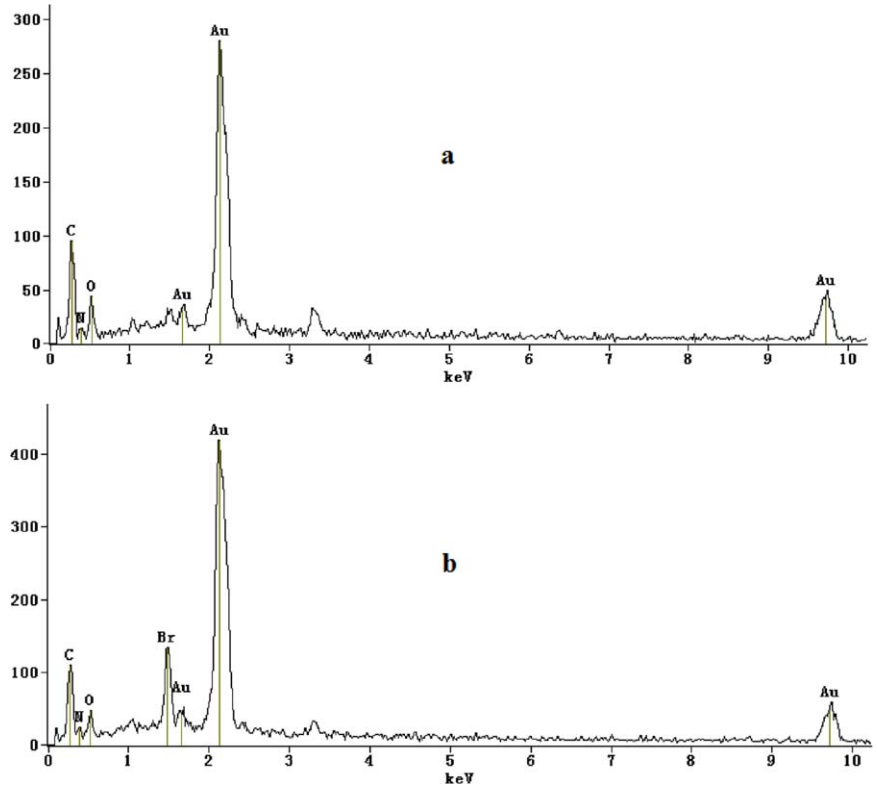

Figure 2. EDS images of active yeast (a) and yeast@Br (b). [Color figure can be viewed in the online issue, which is available at wileyonlinelibrary.com.]

of more than 200 representative particles in the SEM by the ruler. The average particle sizes were calculated as follows:

$$\text{Average particle size} = \sum \text{particle size} \times \text{particle number percentage.}$$

The mean diameter of yeast particles [Figure 3(a)] is 3.77 μm by calculation according to the weighted-averages method. In the same way, the calculated mean diameter of yeast@MIPs [Figure 3(c)] is 4.5 μm. By subtracting calculation the mean diameter of yeast@MIPs and yeast particles, we obtain a difference value 0.73 μm, which is double thickness of MIPs. Thus, we can calculate the mean thickness of the outer MIPs coating layer is 365 nm. Therefore, these results indicated that the surface molecularly imprinted polymers by ATREP exhibited better dispersity and much thicker imprinting layer.

The FT-IR spectra of active yeast, yeast@Br, and yeast@MIPs were shown in Figure 4. A broad absorption band at 3290, 2930, and 1660 cm^{-1} of the active yeast contributed to the stretching vibration of N—H, O—H and C═O bonds, which indicated the presence of abundant functional groups on to the surface of yeast.[39] When comparing with active yeast, the new peaks at 1380 and 1650 cm^{-1} of yeast@Br were assigned to the C—H binding vibrations in isopropyl group and the N—H binding vibrations in amide group, correspondingly. These results demonstrated that the ATRP initiator was effectively immobilized on the surface of active yeast. The yeast@MIPs displayed distinctive peaks around 1727, 1160, and 1050 cm^{-1}, which were ascribed to C═O stretching vibration of carboxyl (MAA, HEMA), C—O symmetric and asymmetric stretching vibrations of ester (EGDMA), respectively.[40] All the results suggested that the ATREP imprinted polymers were successfully synthesized on to the surface of yeast.

Adsorption Isotherm

To demonstrate the binding properties of yeast@MIPs and yeast@NIPs for CIP, the most commonly used models of Langmuir and the Freundlich equations were applied to analyze the experimental data.[41,42] The Langmuir adsorption isotherm model assumes that the adsorption process is conducted only in the surface of adsorbent, with the same combination of monolayer adsorption sites. The Langmuir nonlinear equation is expressed as following:

$$Q_e = \frac{K_L Q_m C_e}{1 + K_L C_e} \tag{6}$$

which can be rearranged to a linear form:

$$\frac{C_e}{Q_e} = \frac{1}{K_L Q_m} + \frac{C_e}{Q_m} \tag{7}$$

The Freundlich adsorption isotherm model supposes that the adsorption process is a multilayer adsorption, nonlinear and linear equations are as follows:

$$Q_e = K_F C_e^{1/n} \tag{8}$$

$$\ln Q_e = \ln K_F + \left(\frac{1}{n}\right) \ln C_e \tag{9}$$

In the above equations, C_e is the equilibrium concentration of adsorbate (mg g^{-1}), Q_e is the equilibrium adsorption capacity (mg g^{-1}), Q_m (mg g^{-1}) is the maximum adsorption capacity of

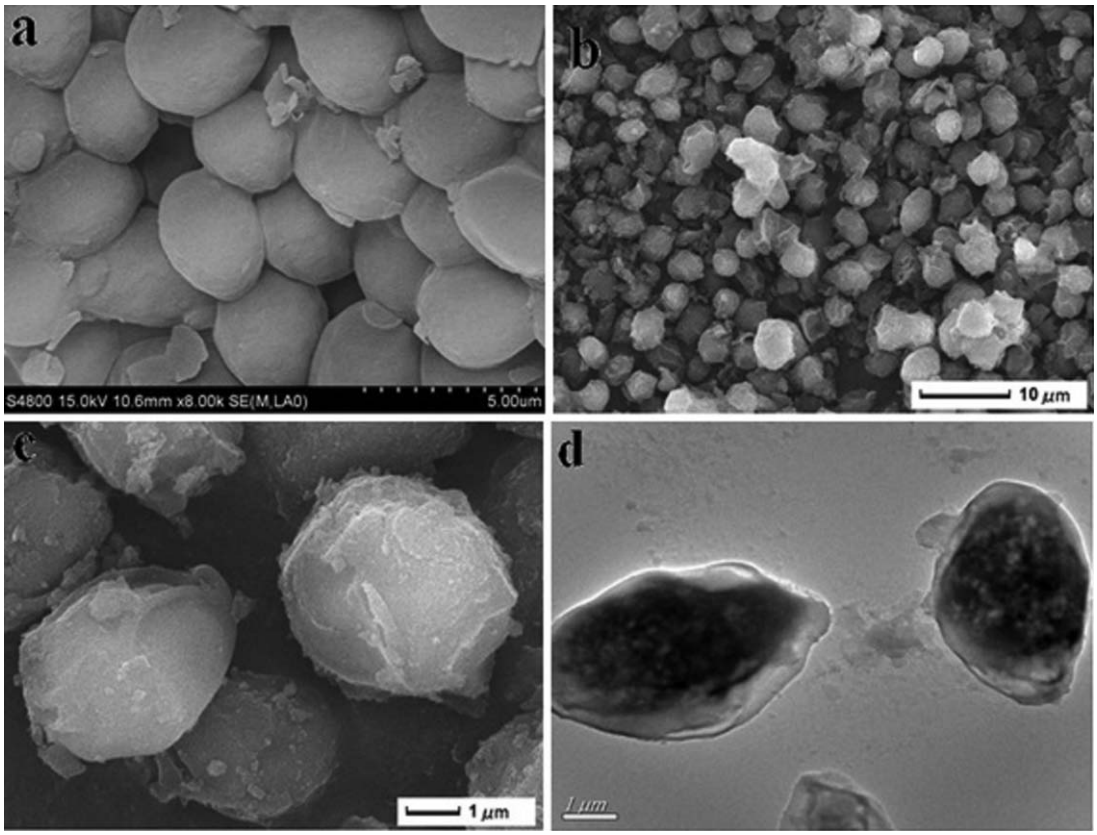

Figure 3. SEM images of yeast (a), yeast@MIPs (b, c), and TEM image of yeast@MIPs (d).

the adsorbent, K_L is the Langmuir affinity constant, K_F and n are both the Freundlich adsorption equilibrium constant. R_L, a dimensionless constant called the equilibrium parameter to measure the Langmuir which is defined as:

$$R_L = \frac{1}{1 + C_m K_L} \tag{10}$$

where C_m (mg L^{-1}) is the maximal initial concentration of CIP. When $0 < R_L < 1.0$, it represents that the isothermal system is favorable adsorption. In addition, the nonlinear curve fit of Langmuir and Freundlich isotherm models for yeast@MIPs and yeast@NIPs were illustrated in Figure 5(a,b) and correlation index constants were apparently acquired in Table II. Moreover, the comparison of adsorption capacity between MIPs and yeast@MIPs was shown in Supporting Information Figure S4.

As illustrated in Figure 5, with the increase in initial concentration, the equilibrium adsorption capacity (Q_e) for CIP increased

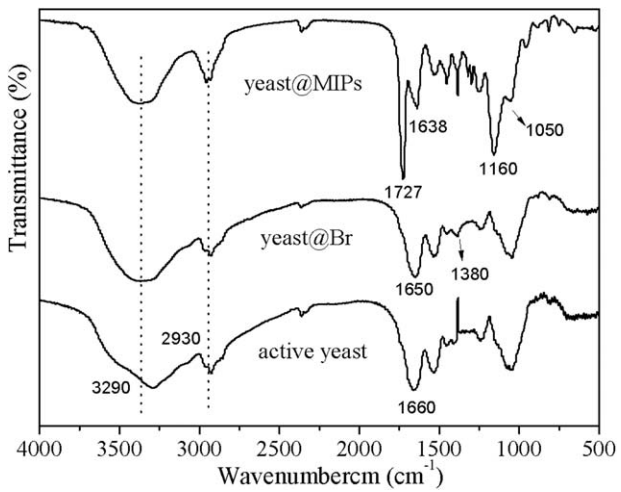

Figure 4. FT-IR spectra of active yeast, yeast@Br and yeast@MIPs.

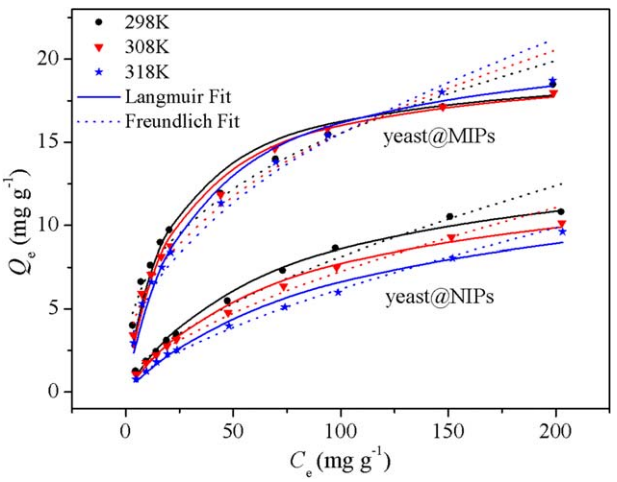

Figure 5. Comparison of Langmuir, Freundlich isotherm models for CIP adsorption on to yeast@MIPs (a) and yeast@NIPs (b) at 298, 308, and 318 K. [Color figure can be viewed in the online issue, which is available at wileyonlinelibrary.com.]

Table II. Langmuir and Freundlich Adsorption Isotherm Constants for CIP on to the Yeast@MIPs and Yeast@NIPs at 298, 308, and 318 K

		Langmuir				Freundlich		
Adsorbents	T (K)	Q_m (mg g^{-1})	K_L (L mg^{-1})	R_L	R^2	K_F (mg g^{-1})	$1/n$	R^2
Yeast@MIPs	298	19.61	0.0503	0.0872	0.9919	3.172	0.3465	0.9749
Yeast@NIPs	298	14.47	0.0150	0.2422	0.9835	0.5147	0.6005	0.9920
Yeast@MIPs	308	19.72	0.0448	0.0969	0.9966	2.527	0.3955	0.9696
Yeast@NIPs	308	13.39	0.0140	0.2555	0.9798	0.4522	0.6036	0.9961
Yeast@MIPs	318	21.14	0.0337	0.1247	0.9925	2.030	0.4431	0.9747
Yeast@NIPs	318	13.37	0.0100	0.3240	0.9523	0.2930	0.6636	0.9960

Table III. Kinetic Parameters for the Pseudo-First-Order and Pseudo-Second-Order Equations

	Pseudo-first-order model				Pseudo-second-order model		
Adsorbents	$Q_{e,exp}$ (mg g^{-1})	$Q_{e,c}$ (mg g^{-1})	k_1 (min^{-1})	R^2	$Q_{e,c}$ (mg g^{-1})	k_2 (g mg^{-1} min^{-1})	R^2
Yeast@MIPs	11.67	11.37	0.3512	0.6232	11.62	0.07652	0.9558
Yeast@NIPs	6.761	6.316	0.1542	0.7227	6.647	0.03750	0.9509

apparently at first, then increased slightly, and finally reached to anticipated equilibrium. As shown in Table II, the maximum adsorption capacity of yeast@MIPs at 298, 308, and 318 K were 19.61, 19.72, and 21.14 mg g^{-1} while that of yeast@NIPs were 14.47, 13.39, and 13.37 mg g^{-1}, respectively. The yeast@MIPs exhibited much higher binding amounts than yeast@NIPs, indicating that specific recognition sites were generated on the surface of yeast@MIPs. Besides, the R_L values ($0 < R_L < 1$) and the Freundlich constant $1/n$ (ranging between 0 and 1) shown in Table II indicated that the experiment conditions were favorable for the adsorption of CIP. Furthermore, the equilibrium adsorption of yeast@MIPs was less affected by temperature varying from 298 to 318 K, which indicated that the proposed method was applicable in preparing more favorable molecularly imprinted polymers of thermal stability performance. Finally, as can be illustrated in Supporting Information Figure S4, yeast@MIPs exhibited much higher binding amounts than MIPs as the initial concentration of CIP increasing. In addition, the morphologies of yeast@MIPs presented better dispersion than MIPs (Supporting Information Figure S3). These results demonstrated that yeast@MIPs had superior performance to MIPs, for the reasons of a variety of specific recognition sites generating on the surface of yeast@MIPs.

Adsorption Kinetics

The kinetic adsorption is important because it controls the performance of the adsorbent.[43] Usually, the pseudo-first-order and pseudo-second-order kinetic model are applied to investigate the controlling mechanisms on to imprinted polymers, which can be expressed as *eqs.* (11) and (12), respectively:

$$Q_t = Q_e - Q_e e^{-k_1 t} \tag{11}$$

$$Q_t = \frac{k_2 Q_e^2 t}{1 + k_2 Q_e t} \tag{12}$$

The above two equations can be transformed into linear forms as follows:

$$\ln (Q_e - Q_t) = \ln Q_e - k_1 t \tag{13}$$

$$\frac{t}{Q_t} = \frac{1}{k_2 Q_e^2} + \frac{t}{Q_e} \tag{14}$$

where Q_e (mg g^{-1}) and Q_t (mg g^{-1}) are the amounts adsorbed of CIP at equilibrium and time t, respectively, k_1 (min^{-1}) is the pseudo-first-order rate constant of adsorption, while k_2 (g mg^{-1} min^{-1}) is the rate constant of pseudo-second-order adsorption. The adsorption kinetics constants and nonlinear regression values of the two models were listed in Table III. It could be seen from Table III that all of R^2 values of this adsorption process on the yeast@MIPs or yeast@NIPs by pseudo-second-order kinetic model were higher than that by pseudo-first-order model. The binding data were well fitted to the pseudo-second-order kinetic model, indicating chemical process was the rate-limiting step in this adsorption kinetic process. The nonlinear and linear regression plots of the pseudo-second-order were shown in Figure 6.

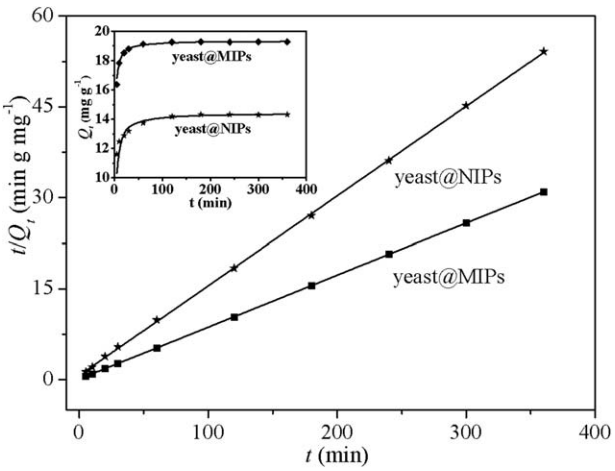

Figure 6. Analysis of kinetics by linear regression fit using a pseudo-second-order kinetic model; the nonlinear dynamic curves of CIP adsorption of yeast@MIPs and yeast@NIPs (inset).

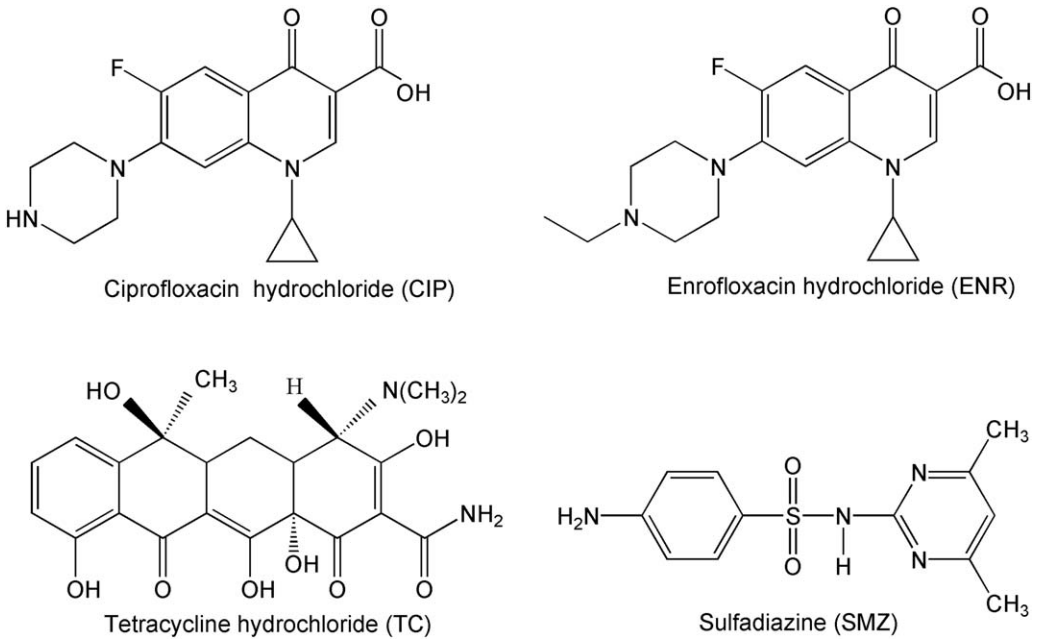

Figure 7. Structure formulas of CIP and three competitive antibiotics.

As could be observed in Figure 6, the inset nonlinear dynamic curves indicated that the adsorption rose speedy in the first 60 min, then grown slowly and eventually reached equilibrium. When comparing with conventional bulk technique (about 5 h),[27] this reasonably rapid binding process was attributed to the presence of a big mass of accessible high-affinity binding sites on the surface of the yeast. It was clearly observed that the adsorption capacity of yeast@MIPs was relatively larger than yeast@NIPs at the same time. Furthermore, the experimental data of adsorption of CIP fitted to the pseudo-second-order quite well because of the encouraging conformity to calculated values of Q_e ($R^2 > 0.99$). All the above results indicated that the presence of specific binding sites on the surface of yeast@MIPs.

Selectivity Study

To gain further insight into the yeast@MIPs, structural analogue ENR and two reference compounds TC, SMZ (Figure 7) were selected to estimate the selective recognition of the CIP. The initial concentrations of CIP, ENR, TC, and SMZ used were all 50 μmol L^{-1} and the batch mode binding experiments were carried out under the same conditions. As shown in Figure 8, yeast@MIPs exhibited the highest selectivity for CIP than the remaining three competitive antibiotics. At the same time, all the compounds being evaluated exhibited much larger binding capability to the yeast@MIPs particles than those of yeast@NIPs. Except for an extra ethyl, ENR had almost the same molecule structure as CIP, but the yeast@MIPs could still specifically recognize the template CIP, which indicated the important role of specific conformation memory in molecular imprinting technique. In addition, the values of K_D, k, and k' were also summarized in Table IV. From the data in Table IV, we could draw the following results: (i) the values of K_D and k of yeast@MIPs presented significant increase than those of yeast@NIPs, suggesting yeast@MIPs had the highest selective binding ability to CIP. (ii) The values of k' for ENR, TC, and SMZ were 1.052, 1.125, and 1.653, respectively, indicating the recognition for competitive compounds followed the order CIP > SMZ > TC > ENR. All these results illustrated that the success of the imprinting process, and we could safely draw a conclusion that yeast@MIPs

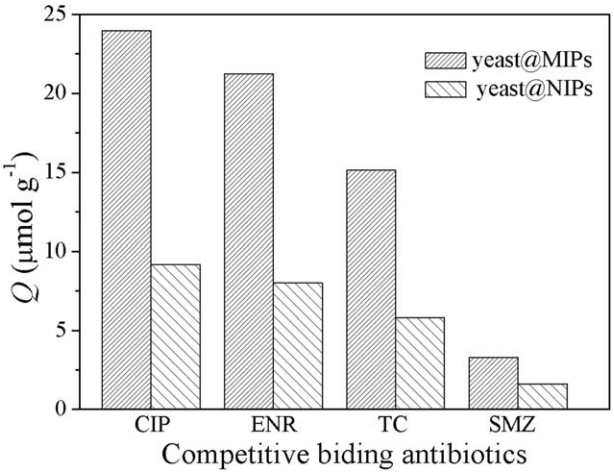

Figure 8. Selective binding analysis of CIP, ENR, TC, and SMZ.

Table IV. Selective Recognition of CIP on to the Yeast@MIPs and Yeast@NIPs

	Yeast@MIPs		Yeast@NIPs		
Antibiotics	K_D (L g^{-1})	K	K_D (L g^{-1})	K	k'
CIP	0.7667	-	0.2338	-	-
ENR	0.6327	1.212	0.2029	1.152	1.052
TC	0.3830	2.002	0.1314	1.779	1.125
SMZ	0.0720	10.65	0.0363	6.441	1.653

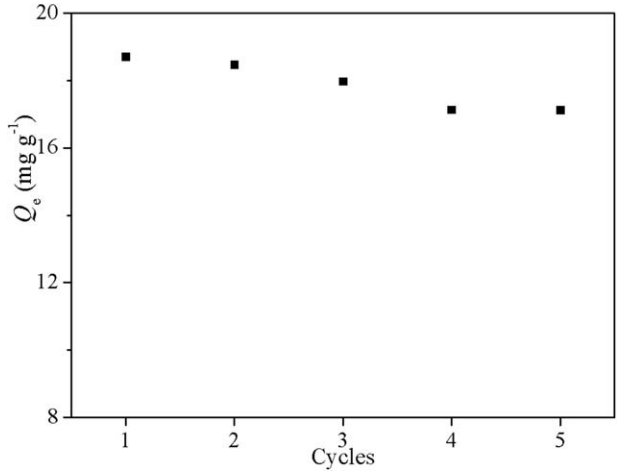

Figure 9. Adsorption capacity of yeast@MIPs for CIP in five adsorption–regeneration cycles.

had expected high-quality selectivity in the presence of other competitive antibiotics.

Desorption and Reuse

With the methanol/acetic acid mixture as desorption agent, the regenerated yeast@MIPs were used to adsorb CIP in subsequent cycle. The adsorption capacity of the yeast@MIPs for CIP with five times was shown in Figure 9. It was clearly seen that yeast@MIPs could be effectively regenerated for further use with only about 8.52% loss of initial binding capacity after five cycles. It was reasonable to assume that the yeast@MIPs could be reused at least five times without decreasing their adsorption capacities significantly.

Analysis of CIP in Shrimp Samples

To further demonstrate the applicability of the yeast@MIPs for the analysis of real samples, the shrimp samples spiked with CIP at 50 μg L^{-1} were detected. As can be clearly seen from Figure 10, the target CIP was not detected in the shrimp samples because of its low concentration. However, the peak around 5.5 min of CIP sharply increased after extraction by yeast@MIPs while yeast@NIPs showed

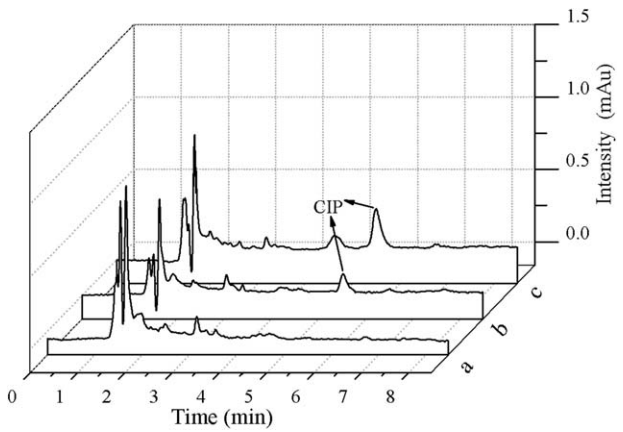

Figure 10. HPLC chromatograms of CIP obtained from (a) spiked shrimp samples, (b) extraction with yeast@NIPs, and (c) extraction with yeast@MIPs. Column: C18 (150 × 4.6 mm^2), mobile phase: methanol–water (24:76, v/v), flow rate: 1.0 mL min^{-1}, detection: 276 nm.

only a small quantity of CIP detected, which was attribute to the absence of specific binding sites on yeast@NIPs. Furthermore, the recovery was 86.4% by analysis of CIP spiked shrimp samples. These results demonstrated that the yeast@MIPs could be applied to trace analysis of CIP in real samples.

CONCLUSIONS

In this work, the novel imprinted polymer was prepared on to the surface of the biological material (yeast) for the selective recognition and removal of targeting ciprofloxacin from aqueous media via ATREP. Based on the advantages of abundant groups on to the surface of yeast, the yeast@Br was synthesized by one step, which was of lower energy consumption and high efficiency compared with multistep traditional ATRP polymers. The prepared surface imprinted yeast@MIPs exhibited high adsorption capacity, fast binding ability, and high selectivity for CIP. The yeast@MIPs could be used at least five times without weakening the adsorption capacity significantly. Moreover, the yeast@MIPs were used to trace analysis of the CIP by HPLC in real samples with satisfactory recoveries.

ACKNOWLEDGMENTS

This work was financially supported by the National Natural Science Foundation of China (No. 21077046, No. 21176107, No. 21174057, No. 21107037, and No. 21277063), the National Basic Research Program of China (973 Program, 2012CB821500), and PhD Innovation Programs Foundation of Jiangsu Province (No. CXZZ13_0668).

REFERENCES

1. Yang, R.; Fu, Y.; Li, L. D.; Liu, J. M. *Spectrochim. Acta, Part A.* **2003**, *59*, 2723.
2. Prieto, A.; Möder, M.; Rodil, R.; Adrian, L.; Marco-Urrea, E. *Bioresour. Technol.* **2011**, *102*, 10987.
3. Sun, H. W.; Qiao, F. X.; Liu, G. Y.; Liang, S. X. *Anal. Chim. Acta.* **2008**, *625*, 154.
4. Tan, F.; Sun, D. M.; Gao, J. S.; Zhao, Q.; Wang, X. C.; Teng, F.; Quan, X.; Chen, J. W. *J. Hazard. Mater.* **2013**, *244–245*, 750.
5. Cazedey, E. C. L.; Salgado, H. R. N. *J. Pharm. Anal.* **2013**, doi:10.1016/j.jpha.2013.03.07.
6. Zheng, M. M.; Gong, R.; Zhao, X.; Feng, Y. Q. *J. Chromatogr. A.* **2010**, *1217*, 2075.
7. Dai, J. D.; Pan, J. M.; Xu, L. C.; Li, X. X.; Zhou, Z.; Zhang, R. X.; Yan, Y. S. *J. Hazard. Mater.* **2012**, *205–206*, 179.
8. Xu, L. C.; Pan, J. M.; Dai, J. D.; Li, X. X.; Hang, H.; Cao, Z. J.; Yan, Y. *J. Hazard. Mater.* **2012**, *48*, 233.
9. Liu, Y. L.; Huang, Y. Y.; Liu, J. Z.; Wang, W. Z.; Liu, G. Q.; Zhao, R. *J. Chromatogr. A* **2012**, *1246*, 15.
10. Golet, E. M.; Alder, A. C.; Hartmann, A.; Ternes, T. A.; Giger, W. *Anal. Chem.* **2001**, *73*, 3632.
11. Lara, F. J.; García-Campaña, A. M.; Alés-Barrero, F.; Bosque-Sendra, J. M.; García-Ayuso, L. E. *Anal. Chem.* **2006**, *78*, 7665.

12. Trivedi, P.; Vasudevan, D. *Environ. Sci. Technol.* **2007**, *41*, 3153.
13. Pan, J. M.; Wang, B.; Dai, J. D.; Dai, X. H.; Hang, H.; Ou, H. X.; Yan, Y. *J. Mater. Chem.* **2012**, *22*, 3360.
14. Guo, W. L.; Hu, W.; Pan, J. M.; Zhou, H.; Guan, W.; Wang, X.; Dai, J. D.; Xu, L. C. *Chem. Eng. J.* **2011**,*171*, 603.
15. Wang, X.; Pan, J. M.; Guan, W.; Dai, J. D.; Zou, X. H.; Yan, Y.; Li, C. X.; Hu, W. *J. Chem. Eng. Data.* **2011**, *56*, 2793.
16. He, M. Q.; Meng, M. J.; Wan, J. H.; He, J.; Yan, Y. S. *Polym. Bull.* **2011**, *68*, 1039.
17. Guan, W.; Pan, J. M.; Ou, H. X.; Wang, X.; Zou, X. H.; Hu, W.; Li, C. X.; Wu, X. Y. *Chem. Eng. J.* **2011**, *167*, 215.
18. Wang, H. J.; Zhou, W. H.; Yin, X. F.; Zhuang, Z. X.; Yang, H. H.; Wang, X. R. *J. Am. Chem. Soc.* **2006**, *128*, 15954.
19. Novoselov, K. S.; Geim, A. K.; Morozov, S. V.; Jiang, D.; Katsnelson, M. I.; Grigorieva, I. V.; Dubonos, S. V.; Firsov, A. A. *Nature* **2005**, *438*, 197.
20. Zhu, G. F.; Fan, J.; Gao, Y. B.; Gao, X.; Wang, J. *J. Talanta* **2011**, *84*, 1124.
21. Zhang, W.; Qin, L.; He, X. W.; Li, W. Y.; Zhang, Y. K. *J. Chromatogr. A* **2009**, *1216*, 4560.
22. Zhu, R.; Zhao, W.; Zhai, M. J.; Wei, F. D.; Cai, Z.; Sheng, N.; Hu, Q. *Anal. Chim. Acta.* **2010**, *658*, 209.
23. Guo, X. M.; Liu, X. G.; Xu, B. S.; Dou, T. *Colloids Surf. A* **2009**, *345*, 141.
24. Ji, J.; Sun, X. L.; Tian, X. M.; Li, Z. J.; Zhang, Y. Z. *Anal. Lett.* **2012**, *46*, 969.
25. Schirhagl, R.; Latif, U.; Dickert, F. L. *J. Mater. Chem.* **2011**, *21*, 14594.
26. Schirhagl, R.; Latif, U.; Podlipna, D.; Blumenstock, H.; Dickert, F. L. *Anal. Chem.* **2012**, *84*, 3908.
27. Zu, B. Y.; Pan, G. Q.; Guo, X. Z.; Zhang, Y.; Zhang, H. Q. *J. Polym. Sci., Part A: Polym. Chem.* **2009**, *47*, 3257.
28. Zu, B. Y.; Zhang, Y.; Guo, X. Z.; Zhang, H. Q. *J. Polym. Sci. Part A Polym. Chem.* **2010**, *48*, 532.
29. Li, C. Y.; Xu, F. J.; Yang, W. T. *Langmuir* **2012**, *29*, 1541.
30. Zhao, N.; Chen, C. B.; Zhou, J. *Sens. Actuat. B: Chem.* **2012**, *166–167*, 473.
31. Lu, C. H.; Wang, Y.; Li, Y.; Yang, H. H.; Chen, X.; Wang, X. R. *J. Mater. Chem.* **2009**, *19*, 1077.
32. Li, Y.; Li, X.; Chu, J.; Dong, C. K.; Qi, J. Y.; Yuan, Y. X. *Environ. Pollut.* **2010**, *158*, 2317.
33. Li, X. X.; Pan, J. M.; Dai, J. D.; Dai, X. H.; Xu, L. C.; Wei, X.; Hang, H.; Li, C. B.; Liu, Y. *Chem. Eng. J.* **2012**, *503*, 198.
34. Li, X. X.; Pan, J. M.; Dai, J. D.; Dai, X. H.; Ou, H. X.; Xu, L. C.; Li, C. X.; Zhang, R. X. *J. Sep. Sci.* **2012**, *35*, 2787.
35. Fonseca, G. E.; McKenna, T. F.; Dubé, M. A. *Chem. Eng. Sci.* **2010**, *65*, 2797.
36. Zou, X. H.; Pan, J. M.; Ou, H. X.; Wang, X.; Guan, W.; Li, C. X.; Yan, Y.; Duan, Y. Q. *Chem. Eng. J.* **2011**, *167*, 112.
37. Pan, J. M.; Zou, X. H.; Wang, X.; Guan, W.; Yan, Y.; Han, J. *Chem. Eng. J.* **2010**, *162*, 910.
38. Yan, Y.; Sun, S. F.; Song, Y.; Yan, X.; Guan, W. S.; Liu, X. L.; Shi, W. D. *J. Hazard. Mater.* **2013**, *250–251*, 106.
39. Meng, M. J.; Wang, Z. P.; Ma, L. L.; Zhang, M.; Wang, J.; Dai, X. H.; Yan, Y. *Ind. Eng. Chem. Res.* **2012**, *51*, 14915.
40. Yoshimatsu, K.; Reimhult, K.; Krozer, A.; Mosbach, K.; Sode, K.; Ye, L. *Anal. Chim. Acta.* **2007**, *584*, 112.
41. Mazzotti, M. *J. Chromatogr. A* **2006**, *1126*, 311.
42. Allen, S. J.; McKay, G.; Porter, J. F. *J. Colloid Interface Sci.* **2004**, *280*, 322.
43. Ho, Y. S.; McKay, G. *Process Biochem.* **1999**, *34*, 451.